Aircraft Flight Envelope Determination using Upset Detection and Physical Modeling Methods

Jeffrey D. Keller[1], Robert M. McKillip, Jr.[2]
Continuum Dynamics, Inc., Ewing, NJ, 08618

and

Sungwan Kim[3]
NASA Langley Research Center, Hampton, VA, 23681

The development of flight control systems to enhance aircraft safety during periods of vehicle impairment or degraded operations has been the focus of extensive work in recent years. Conditions adversely affecting aircraft flight operations and safety may result from a number of causes, including environmental disturbances, degraded flight operations, and aerodynamic upsets. To enhance the effectiveness of adaptive and envelope limiting controls systems, it is desirable to examine methods for identifying the occurrence of anomalous conditions and for assessing the impact of these conditions on the aircraft operational limits. This paper describes initial work performed toward this end, examining the use of fault detection methods applied to the aircraft for aerodynamic performance degradation identification and model-based methods for envelope prediction. Results are presented in which a model-based fault detection filter is applied to the identification of aircraft control surface and stall departure failures/upsets. This application is supported by a distributed loading aerodynamics formulation for the flight dynamics system reference model. Extensions for estimating the flight envelope due to generalized aerodynamic performance degradation are also described.

I. Introduction

TECHNOLOGY advancements have resulted in significant reductions in fatal aircraft accidents in recent years, although it is always desirable to seek cost-effective ways to further enhance aviation safety. With the expected growth in air traffic capacity as part of the Next Generation Air Transportation System (NextGen), improving the inherent safety for all aircraft operations has been and continues to be an active area of research and development. To have continuing impact on safety, improvements must address the leading causes of aircraft accidents, which historically have been controlled flight into terrain (CFIT) and loss of control in-flight (LOC-I). Aircraft accident data surveys have shown that LOC-I accidents between 1987 and 2005 have resulted in more than 2800 fatalities worldwide[1,2]. While there may be several contributing factors in any single LOC-I accident, the primary causes can be attributed to environmental effects (including both atmospheric and man-made disturbances, such as wake vortex encounters, as well as aircraft icing), subsystem degradation, equipment malfunctions and failures, and piloting error.

While effective pilot training can reduce fatal accident rates associated with LOC-I, flight control developments provide a parallel path for enhancing aircraft safety, in particular when the aircraft is subject to vehicle impairment and/or anomalous flight conditions. Specifically, it is desirable to develop estimation and identification methods to identify/diagnose anomalous conditions and to determine appropriate recovery commands, which can consist of pilot indicators/guidance cueing and/or active feedback/feedforward commands. Some research and development that has been performed in recent years toward this end includes (1) fault detection, isolation, and reconfiguration (FDIR) methods for identifying failures in critical flight control components, such as sensors and actuators, and providing reconfiguration to maintain sufficient closed-loop functionality[3-6]; (2) envelope limiting control systems

[1] Associate, 34 Lexington Ave., Ewing, NJ 08618, AIAA Senior Member.
[2] Senior Associate, 34 Lexington Ave., Ewing, NJ 08618, AIAA Senior Member.
[3] Senior Research Engineer, NASA Langley Research Center, Hampton, VA 23681, AIAA Associate Fellow.

where corrective commands are generated as operational limits are approached to prevent excursions into potentially dangerous flight regimes[7-9]; and (3) adaptive control methods where feedback/feed-forward commands are determined to counteract changes in the aircraft system and/or operational environment[10,11]. Note that this (brief) literature survey is not intended to be comprehensive but is used to indicate the diversity of research and development that has addressed flight control approaches for improving aircraft safety, in particular during degraded flight operations.

Adaptive control technology specifically has received much attention in recent years given its potential for providing resiliency to aircraft system degradation and impairment. Recent flight test demonstrations have shown the potential for improved safety but have also highlighted some potential issues. Specifically, control adaptation schemes may be sensitive to initial pilot reactions following a subsystem failure, which can cause the adaptive controller gains to "over-correct" and/or introduce side effects (in the cross-coupling control/response axes). This behavior was observed in Ref. 10, where the roll axis gains for a precision (pitch axis) tracking task following the failure of one stabilator introduced the tendency for a pilot induced oscillation in one piloted evaluation case. While adaptive control technology offers flexibility, it should be recognized that performance/robustness of the overall system may be improved with outer-loop "supervision" from a system that diagnoses potential impairment in parallel with recovery command generation. This supervision can be used to direct adaptively generated command responses and/or to protect against limit exceedances, which may be radically different for an aircraft that has experienced degradation of one or more critical subsystems.

One approach to enhance the effectiveness of adaptive/envelope limiting flight control systems during vehicle impairment is to incorporate an on-board aircraft flight envelope estimation system in an outer "supervisory" loop. A notional system is illustrated in Fig. 1. On-board flight envelope estimation requires methods for identifying and isolating anomalous conditions and/or vehicle impairment (aerodynamic performance monitoring) that can be used to diagnose the impact of identified aircraft degradation with respect to operational restrictions. Output from the envelope estimation system can be used to augment control loop and/or limit protection gains to ensure that control adaptation for the degraded aircraft does not inadvertently lead to more dangerous flight conditions. Output may also feed guidance command generation to assist in safely landing the (impaired) aircraft.

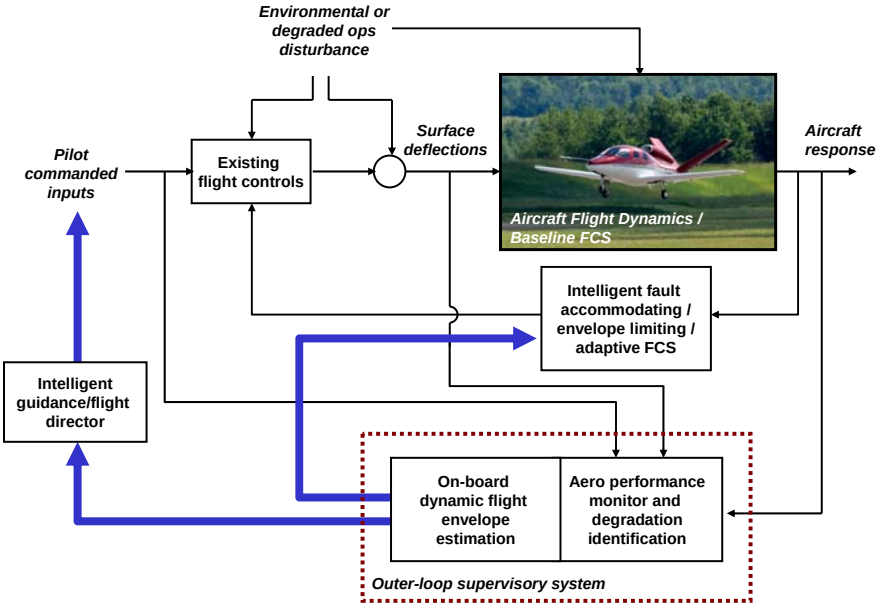

Figure 1. Illustration of Notional On-board Envelope Estimation System as part of an Outer Loop Intelligent Flight Control System

In the following sections of this paper, results from proof-of-concept research and development work are described that examine several aspects of an on-board flight envelope estimation system. Specific areas discussed include the application of fault detection methods applied to the whole aircraft to perform aerodynamic performance and degradation monitoring. The application of a model-based approach for determining the flight envelope subject to vehicle impairment is also provided. Considerations for on-board implementation of an envelope estimation system are discussed, followed by conclusions from this initial work and areas for future development.

II. Fault Detection Methods for Aircraft Performance Degradation Monitoring

The need for reliable methods for fault detection has grown with the increasing complexity of many aerospace systems and the need for reliable operations in potentially challenging environments. The survey paper[6] provides an overview of various FDIR techniques that have been examined over the past decades, with a focus toward model-

based methods that include robust residual generation and statistical decision techniques, in addition to controller reconfiguration methods to accommodate failures when detected. While a broad range of methods have been examined for performing fault diagnostics, model-based methods have the benefit of providing fault diagnostic capabilities with reduced sensing requirements. One class of fault detection methods is based on the use of linear filters – referred to as fault detection filters (FDF) – tailored to identify one or more pre-postulated failure modes[12,13]. The FDF approach (also referred to as the Beard-Jones FDF) provides a means to perform fault detection and isolation using a full state linear observer. The Beard-Jones FDF approach was later extended by Messerole for nonlinear systems[14]. An extensive body of literature exists that considered many aspects of the design and application of filters that have been tailored to respond to pre-defined faults[15-18].

Development of a fault detection filter for a particular application, whether for identifying component failures or for aerodynamic performance degradation as outlined below, follows a similar development strategy for gain selection. The main feature of the method consists of constructing a state estimator for the dynamic system (see Fig. 2) that selects a feedback gain on the measurement residual to make the overall estimator sensitive to pre-specified types of system failures (modes). The magnitude of the residual, which should be zero under normal conditions, indicates the departure of the system from some pre-postulated reference model, due to a failed sensor, actuator, or an unexpected disturbance affecting the dynamic system. The detection filter reference model is formulated as a linear perturbation model, where in state space form is given as follows:

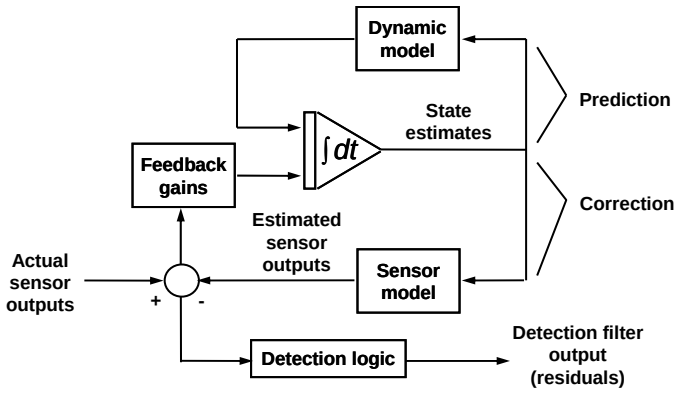

Figure 2. Fault Detection Filter (FDF) Structure for Aircraft Fault (Upset) Detection

$$\begin{aligned} \dot{\mathbf{x}} &= \mathbf{A}\mathbf{x} + \mathbf{B}\mathbf{u} + \sum \mathbf{f_i} n_i(t) \\ \mathbf{y} &= \mathbf{C}\mathbf{x} + \mathbf{D}\mathbf{u} \end{aligned} \tag{1}$$

where $\mathbf{x}$ is the aircraft state vector, $\mathbf{u}$ is a vector of control inputs, and ($\mathbf{A}$, $\mathbf{B}$, $\mathbf{C}$, $\mathbf{D}$) are the linearized system matrices that include terms due to both aerodynamic and inertial effects. The last term in the state rate equation represents the disturbances to the system response that are associated with the aircraft upset state. Note that the constant vector $\mathbf{f_i}$ represents an additive disturbance to the system and is sometimes referred to as the event vector associated with a particular failure mode, and $n_i(t)$ is an arbitrary (scalar) time history. The objective of the detection filter is to choose a full-state observer gain matrix $\mathbf{H}$, i.e.,

$$\begin{aligned} \dot{\hat{\mathbf{x}}} &= \mathbf{A}\hat{\mathbf{x}} + \mathbf{B}\mathbf{u} + \mathbf{H}(\mathbf{y} - \hat{\mathbf{y}}) \\ \hat{\mathbf{y}} &= \mathbf{C}\hat{\mathbf{x}} + \mathbf{D}\mathbf{u} \end{aligned} \tag{2}$$

where $\hat{\mathbf{x}}$ and $\hat{\mathbf{y}}$ are the estimates of the state and output vector so that the filter residual $\mathbf{r}$, defined as:

$$\mathbf{r} = \mathbf{R}(\mathbf{y} - \hat{\mathbf{y}}) \tag{3}$$

maintains a fixed direction in output space ($\mathbf{R}$ is a feed-forward gain matrix that decouples the residual response). Through careful selection of the gain matrices, one may force the measurement residual to remain fixed in a particular direction or a specific plane for a given failure (upset) mode. Note that the review given in Ref. 6 provides additional discussion of alternative methods for residual generation.

While commonly used for detecting and isolating component faults, FDF methods have been previously applied to aerodynamic performance degradation, such as aircraft icing[19-21]. In Ref. 21, a FDF-based algorithmic approach to detect icing conditions was developed for the V-22 tiltrotor aircraft. This approach used a Beard-Jones FDF to

identify and distinguish icing "fault modes" in flight measurements from normal flight operations. This approach provided a method to determine not only if aircraft icing occurred but also the region of the aircraft (wing or proprotor) where significant ice accretion existed. Representative results from this application of fault detection methods to icing detection are illustrated in Fig. 3.

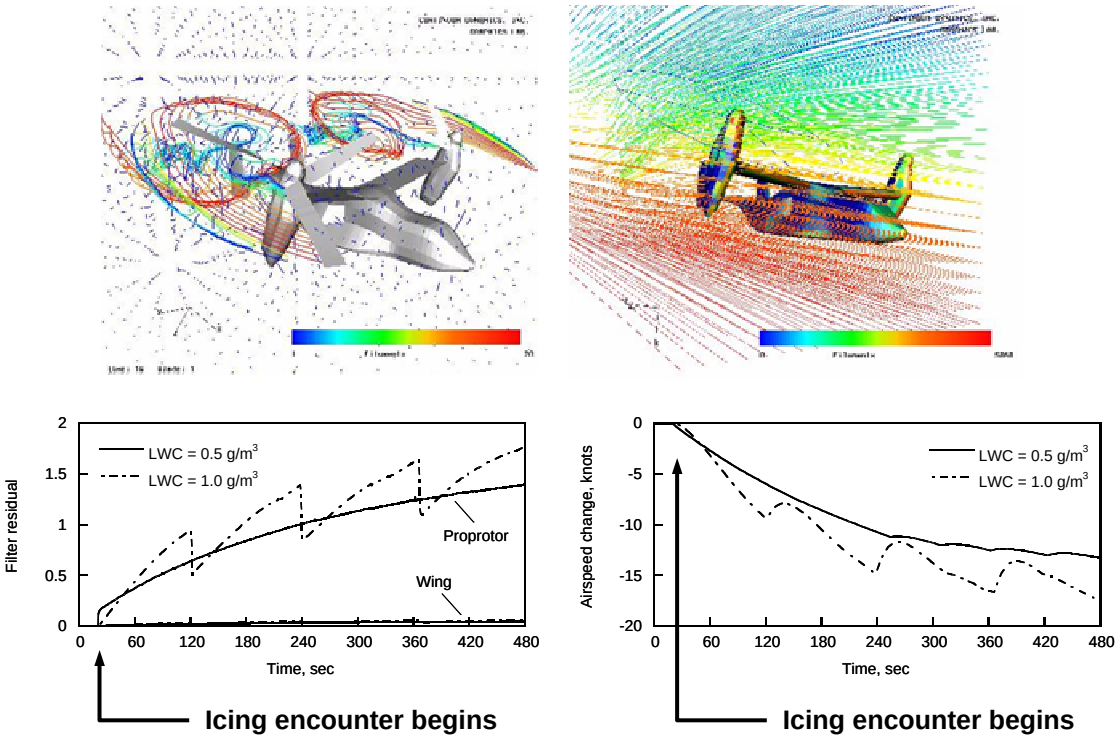

Figure 3. Representative Results for V-22 Aircraft Icing Simulation and FDF-based Icing Detection System; Top – Flow field and droplet trajectory simulation; Bottom – Icing detection filter output.

This approach for aerodynamic performance monitoring has been recently extended to identify the onset of an aircraft upset condition. In this application, pre-postulated upset conditions, such as a stall departure, may be treated as an additional disturbance to the (linear) reference model used to formulate the detection filter. The development of an upset detection filter (UDF) follows from the procedure outlined above. With sufficient available measurements, it should be possible to identify aerodynamic degradation and upset conditions, in addition to control surface failures, as part of an overall performance monitoring system. Results presented in the following section describe initial work performed to demonstrate this application.

III. Aircraft Fault/Upset Detection Development and Demonstration

An overview of initial work on the application of fault detection methods for identifying component failures and the onset of aerodynamic upset conditions is described. This work applied the UDF approach to a small radio-controlled aircraft, which was used to obtain flight test data for evaluating the concept.

A. Flight Test Summary

Flight test data were acquired for a small, unmanned radio-controlled aircraft for evaluation of the UDF approach. The flight test vehicle was the Great Planes Siren commercial almost ready-to-fly (ARF) aircraft (Fig. 4). This aircraft has been used previously as a demonstration platform for a number of applications including distributed, smart material-based actuation concepts and evaluation of flight control and avionics systems. Data from this flight test activity also has been used for validating the distributed aerodynamics loading modeling approach described later in this paper[22].

Figure 4. Great Planes Siren Radio Controlled Aircraft in Flight.

The test aircraft was instrumented with a custom instrumentation package that was used to examine sensor requirements for performing upset detection (and recovery). This instrumentation package (illustrated schematically in Fig. 5) consisted of the following components: a five degree of freedom (DOF) MEMS inertial measurement unit (IMU) consisting of a two-axis, vibrating mass rate gyro (InvenSense IDG-300) and a three-axis accelerometer (Analog Devices ADXL330); a patch-size GPS receiver (Grand Idea Studio/Parallax) with 1 Hz update rate; a 900 MHz radio transmitter/receiver telemetry link (MaxStream 9XStream) with 19.2 kbaud serial output capability; and two PIC 16F690 microcontroller units (MCU) that provided data sampling and serial output capabilities. Note that one microcontroller has been designated the master MCU, which provides analog-to-digital conversions of the IMU rate gyros (pitch and roll rate) and three-axis accelerometers, in addition to coordinating the serial output across a single "party line" through the telemetry link to the ground station. The other microcontroller has been dedicated to reading and parsing the NMEA sentences from the GPS receiver, providing output of the GPS satellite time, latitude, longitude, and altitude, as well as the course speed and heading.

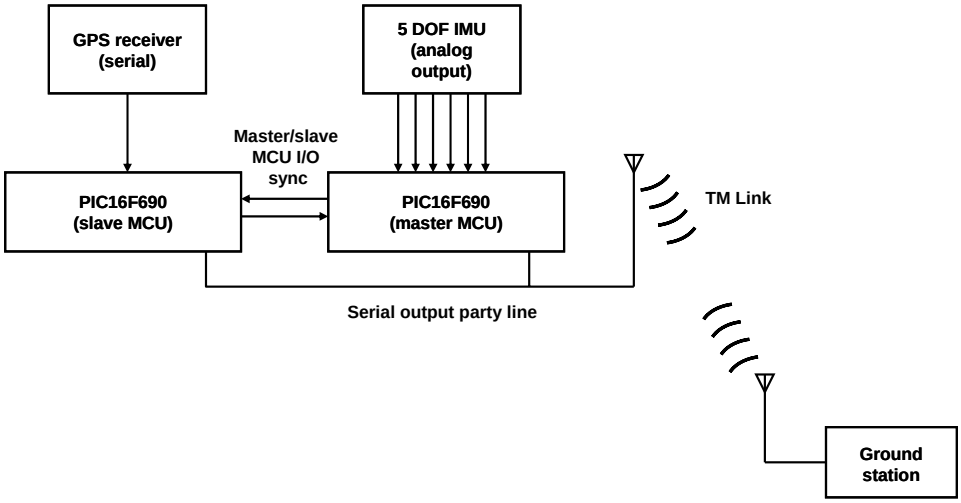

Figure 5. Schematic Illustration of Flight Instrumentation Package.

Several flights were performed to obtain data to define flight dynamics characteristics during nominal flight conditions and stall encounters. Data were also acquired during one flight with a gain reduction on the left aileron servo to simulate an actuator failure. Flights were typically performed with the aircraft velocity between 25 to 30 knots (ground speed) and at approximately 100 to 200 feet altitude above ground level. Winds during flight tests were generally light and variable.

Data were telemetered to the ground station and recorded continuously to file during each flight. Inputs from the radio controller were also recorded at the ground station to provide a measurement of the commanded control inputs to the aircraft. The ground station provided a real-time display of the altitude and ground speed from the GPS receiver. The time stamp from the GPS receiver was also displayed at the ground station monitor, which permitted logging of flight maneuvers for data analysis following the test flight. Note that latency was observed between commanded inputs and the aircraft response, which was believed to be caused by delays introduced by the radio uplink/downlink. This latency was removed as part of post-flight data analysis.

Representative flight data are shown in Figs. 6 and 7. Flight test data for a series of lateral pulse inputs, resulting in an "S-turn" maneuver, are shown in Fig. 6. Commanded control inputs are plotted as percentage of total control deflection, where zero corresponds to full left and full aft for the lateral and longitudinal control input. Figure 7 shows flight test data for a power-off stall break (departure) maneuver. During this maneuver, the airspeed was bled off gradually until the aircraft pitched nose down and subsequently rolled to the left. The peak roll rate during the stall break was significant, reaching a maximum of approximately 150 deg/sec. Pilot recovery inputs were not immediately applied during this maneuver to provide data for the aircraft spin recovery characteristics. It was found that the aircraft demonstrated good stability characteristics in the post-stall regime.

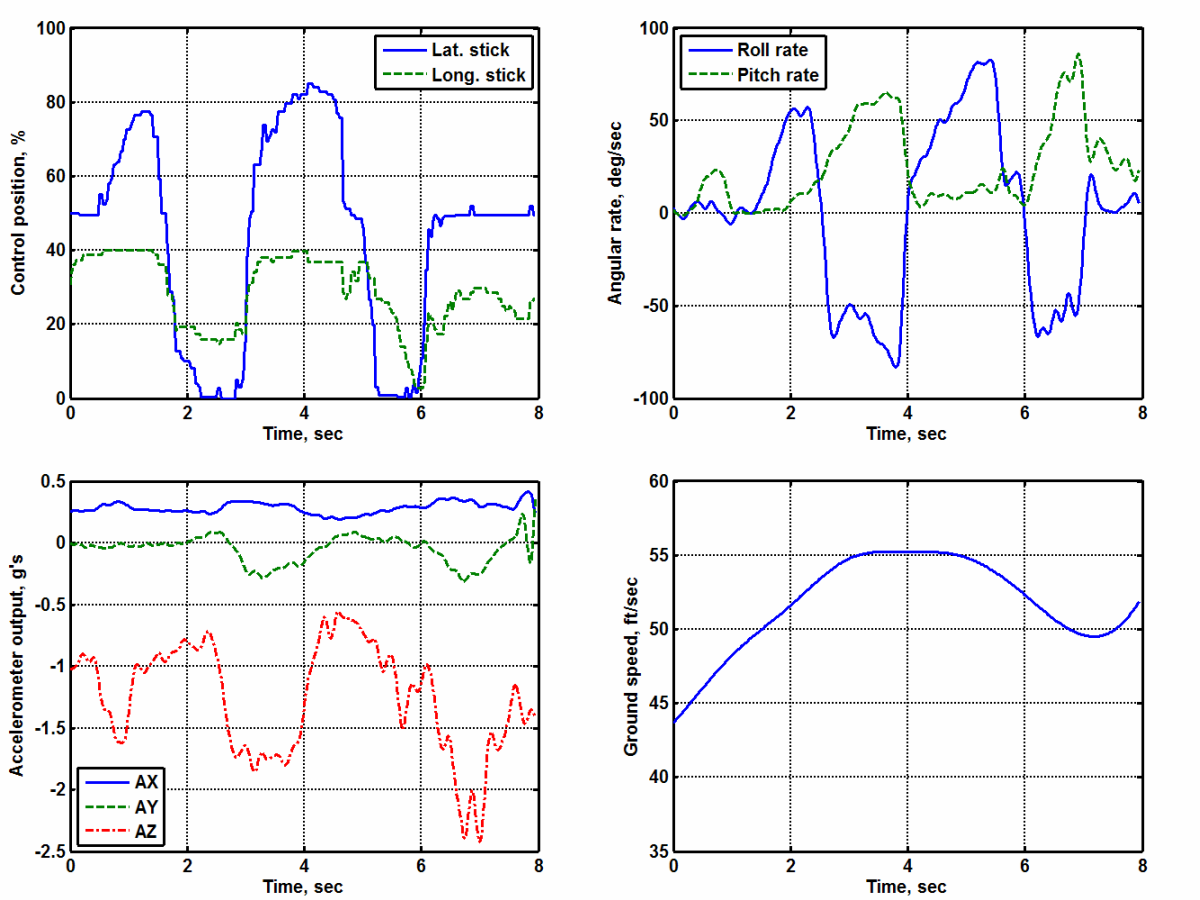

Figure 6. Flight Test Data for S-Turn Lateral Input Maneuver.

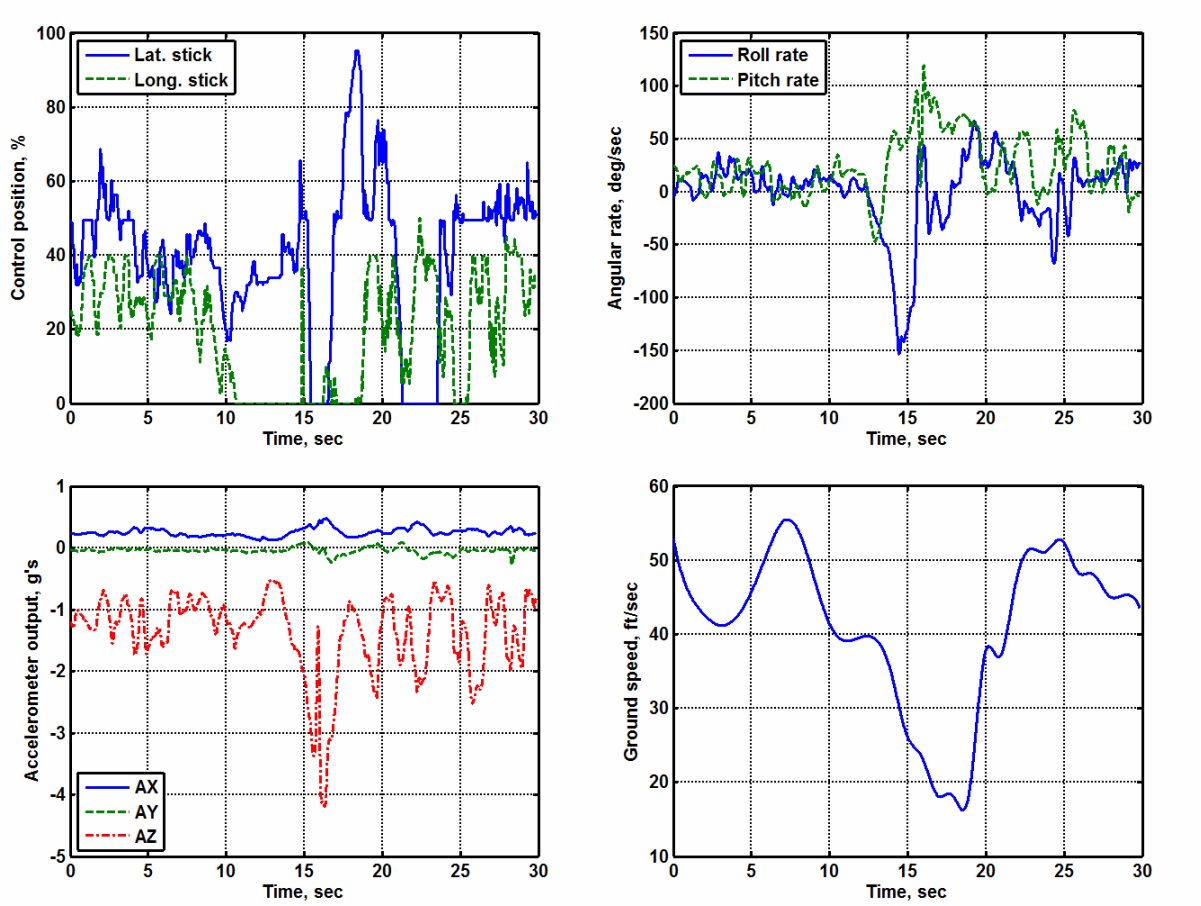

Figure 7. Flight Test Data for Stall Maneuver with Roll Break.

B. Detection Filter Development

The approach described previously was used to develop an UDF for identifying both component (control surface) failures and stall departure (upset). For this application, only output from the MEMS IMU was available (reconstruction of the full state vector from IMU and GPS measurements was not performed). Since available measurements were limited to accelerometer and angular rate measurements only, the UDF was developed using a third order reference model consisting of the fast rigid-body aircraft dynamics (i.e., the short-period pitch dynamics and roll convergence mode). Thus, the linearized reference model is structured as follows:

$$\begin{aligned} \dot{\mathbf{x}} &= \mathbf{A}\mathbf{x} + \mathbf{B}\mathbf{u} \\ \mathbf{y} &= \mathbf{C}\mathbf{x} + \mathbf{D}\mathbf{u} \end{aligned} \tag{4}$$

where the state vector consists of the roll rate, vertical velocity, and pitch rate:

$$\mathbf{x}^T = \begin{bmatrix} p & w & q \end{bmatrix}$$

the control vector consists of the lateral and longitudinal control perturbations:

$$\mathbf{u}^T = \begin{bmatrix} \delta_{lat} & \delta_{lon} \end{bmatrix}$$

and the measurement vector consists of the roll rate, pitch rate, and vertical acceleration:

$$\mathbf{y}^T = \begin{bmatrix} p & q & a_z \end{bmatrix}$$

The linearized system matrices are defined in terms of conventional stability derivatives as follows:

$$\mathbf{A} = \begin{bmatrix} L_p & 0 & 0 \\ 0 & Z_w & U_o \\ 0 & M_w & M_q \end{bmatrix}$$

$$\mathbf{B} = \begin{bmatrix} L_{lat} & 0 \\ 0 & Z_{lon} \\ 0 & M_{lon} \end{bmatrix}$$

$$\mathbf{C} = \begin{bmatrix} 1 & 0 & 0 \\ 0 & 0 & 1 \\ 0 & Z_w & 0 \end{bmatrix}$$

$$\mathbf{D} = \begin{bmatrix} 0 & 0 \\ 0 & 0 \\ Z_{lon} & 0 \end{bmatrix} \tag{5}$$

where U_o is the trim longitudinal velocity and the remaining terms in Eq. (5) are the (dimensional) stability derivatives. Reference model parameters (stability derivatives) were determined from a nonlinear simulation of the aircraft using linear perturbation analysis around a 30-knot trim flight condition.

Since the short period dynamics are affected by the aircraft lift curve slope (through the Z_w stability derivative), it is possible to detect the onset of (asymmetric) stall conditions. A detection filter was developed to identify the onset of a stall departure, as well as an aileron servo failure. Development of the detection filter was done by selecting event vectors, i.e., the $\mathbf{f_i}$ terms in Eq. (1), corresponding to these failure modes. For the stall departure mode, a suitable event vector was defined as a disturbance to the Z-force equation, i.e., $\mathbf{f_{stall}^T} = \begin{bmatrix} 0 & 1 & 0 \end{bmatrix}$. The aileron servo failure event vector was defined similarly as a disturbance to the force and moment equations, although this failure mode involved coupling of all degrees of freedom and was aircraft configuration specific. The detection filter gains were determined using eigenstructure assignment design methods, where the remaining closed loop eigenvector was chosen to be orthogonal to the stall and servo failure modes to provide additional robustness. The feed-forward gain matrix $\mathbf{R}$ in Eq. (3) was determined to decouple the filter residuals and to scale the filter response to yield a common detection threshold for each upset mode. It was found that adjustments to the design feed-forward matrix were required to provide detection mode decoupling based on results from the flight test application. The final (single point) design was found to provide detection/isolation of both stall and servo failure modes, while allowing a detection threshold to avoid false positive trips due to maneuvering flight conditions.

C. Results

Results illustrating the performance of this third-order UDF with stall departure and servo failure modes are shown in Figs. 8 through 10. A detection threshold of ±2 is also shown, as indicated by dotted lines in each plot. This threshold was determined to provide failure/upset mode detection without false indications due to maneuvering in non-degraded flight conditions. Figure 8 illustrates the detection filter output for lateral S-turn maneuvers without failed servo (corresponding to Fig. 6). The filter residuals stay below the detection threshold during the maneuver, although each residual can be observed to approach the threshold for segments of the maneuver where maximum lateral control deflection is applied. This maneuver provides a significant test for the detection filter methodology, allowing bounds on the detection thresholds to be set to result in no false positive trips during aggressive maneuvering.

Figure 9 illustrates the detection filter response for lateral maneuvering with failed aileron servo. Although the aileron servo was failed during the entire maneuver, the failed servo mode residual is observed to exceed the

Figure 8. Third Order UDF Output for Lateral S-Turn Maneuver.

Figure 9. Third Order UDF Output for Lateral S-Turn Maneuver with Simulated Failed Aileron Servo.

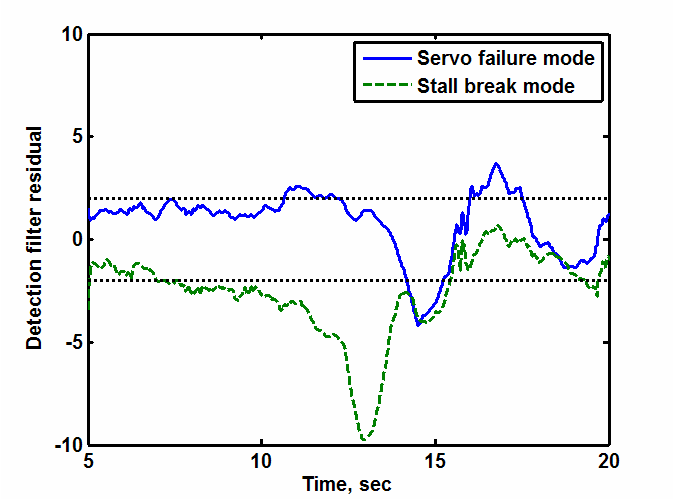

Figure 10. Third Order UDF Output for Stall Departure.

detection threshold only during segments of the maneuver when left stick is applied. The detection filter response is rapid once the roll rate has reversed direction.

Figure 10 illustrates the detection filter response during the stall break encounter (shown in Fig. 7). For this case, the stall mode slowly increases in magnitude as airspeed is reduced and reaches a peak value at approximately 13 seconds, at which point the aircraft experienced the rapid nose down acceleration as the aircraft stalls. For the selected filter gains, the stall mode magnitude exceeds the threshold several seconds before the stall departure occurred. Thus, corrective actions to prevent the stall could be performed prior to the actual break and roll entry.

Results presented in this section demonstrate the feasibility of this algorithmic approach to detecting aircraft component faults and onset of upset conditions. These results were obtained with minimal on-board sensor requirements. The following sections of the paper discuss generalization of these initial results and application to envelope estimation.

IV. Generalized Aerodynamic Performance Degradation and Envelope Estimation

Results in the previous sections indicate that fault detection methods may be effectively applied to detection anomalous conditions affecting the overall aerodynamic performance of an aircraft. The FDF approach has advantages such as the ability to assess anomalous conditions with minimal sensing requirements. To serve as a foundation for an on-board envelope estimation system, however, it is necessary to examine methods to assess the impact of aircraft degradation on the overall aircraft performance and operational limits. Work toward this end is described below, focusing on model-based methods for detecting generalized aerodynamic performance degradation and for analytically determining the flight envelope. The approach is applied for lifting surface damage to a scaled unmanned aircraft as an example demonstration.

A. Distributed Loading Model Formulation

An analytical approach for envelope limit assessment has been examined based on a generic flight dynamics model formulation. This formulation calculates the distributed loading on the aircraft subject to control input and dynamic response characteristics, which is geometry-based in contrast to the conventional data-driven approach typically used in six degree of freedom simulations. This generic aerodynamic and flight dynamics modeling approach has been applied to a range of aircraft configurations with minimal input data requirements. This approach has been developed and documented previously[22]; a brief summary is provided herein.

The distributed loading model formulation provides a generic method for determining the aerodynamic loads on a complete aircraft configuration based on a component build-up approach. The approach is illustrated in Fig. 11, where lifting surfaces are discretized into elements where the local aerodynamic characteristics are approximated as two-dimensional. The sectional lift, drag, and pitching moment can be approximated as functions of the local angle of attack and flap/control surface deflection for low speed flight conditions. For each element, the local angle of attack is determined from the aircraft kinematics, planform geometry, and the induced velocity due to the generation of lift on the each surface. From the local angle of attack distribution across the lifting surface and control surface deflections, if present, the distributed aerodynamic forces (lift, drag, and moment) are calculated, resolved into the aircraft body axis reference frame, and integrated through summation to yield the total aerodynamic loads.

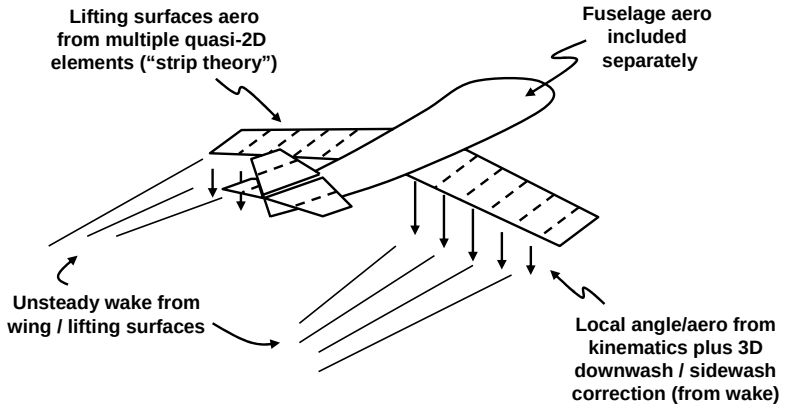

Figure 11. Illustration of Distributed Loading Aerodynamic Model for a Generic Aircraft Configuration.

Note that the distributed loading formulation (also commonly referred to as a strip theory method) forms the basis for at least one commercial flight simulation – X-plane by Laminar Research[23,24]. Distributed loading or strip theory methods are more commonplace in rotorcraft simulations, commonly referred to as blade element methods in the rotary-wing flight simulation community[25].

An advantage of this modeling approach is that input data requirements, in particular aerodynamic data requirements, are greatly reduced. The primary input data includes geometric parameters and sectional aerodynamic data, in addition to other flight dynamics parameters such as mass properties, control system riggings, and propulsion system characteristics). Sectional aerodynamic data, including stall characteristics, are more easily defined than complete aircraft aerodynamic data. When formulating the aerodynamic loads based on two-dimensional sectional data, it is necessary to account for three-dimensional aerodynamic effects explicitly by including a model for the induced downwash and sidewash, which may consist of momentum-based and unsteady wake methods[22]. Momentum-based models are typically adequate for low angles of attack, whereas wake methods would be required to capture aerodynamic and interactional effects associated with large angles of attack and sideslip. Fuselage aerodynamic data are also required as part of the aerodynamic model build-up process, and these data can be derived from conventional stability and control methods (i.e., DATCOM), which are generally sufficient for small angles of attack and sideslip within the normal operating flight envelope. Note that strip theory methods generally have greater applicability to conventional fixed-wing aircraft configurations such as high aspect ratio aircraft that have been examined in this paper. Alternative aerodynamic modeling methods (e.g., vortex lattice models) would be required for more general applicability.

B. Distributed Loading Model Benchmarking

The distributed loading aerodynamic modeling approach has been applied to several aircraft to validate its effectiveness for capturing flight dynamics response characteristics. Recently, the model was applied to the NASA Langley Research Center (LaRC) Generic Transport Model (GTM) configuration as part of additional model benchmarking and validation. The present distributed loading model application used momentum-based methods for modeling the induced velocity rather than an unsteady wake model.

The distributed loading model was applied within a 6 DOF flight dynamics model for the GTM configuration. This application included a model for the propulsive system, control system gearings and limiters, and actuator models, in addition to mass properties representative of the aircraft configuration. Since the airfoil cross-section was not available, generic sectional aerodynamic data were used. Some discrepancies between the LaRC GTM model, which includes polynomial fits for the 6 DOF static and dynamic aerodynamic data derived from wind tunnel testing, and the distributed loading model can be attributed to approximations made with the generic sectional data.

Comparisons between the LaRC GTM and distributed loading models are shown in Figs. 12 and 13, illustrating trim characteristics and dynamic response characteristics, respectively. Initial results (identified as the "Baseline model") indicated some discrepancies between models, and some semi-empirical corrections were applied to the distributed loading model. With corrections, the updated distributed loading model captures the trim characteristics (Fig. 12) predicted by the LaRC GTM model up to the stall speed. Predicted dynamic response characteristics (Fig. 13) are also in good agreement with distributed loading model corrections in place, although some minor discrepancies can be seen in the frequency and damping of the short period and Dutch roll modes.

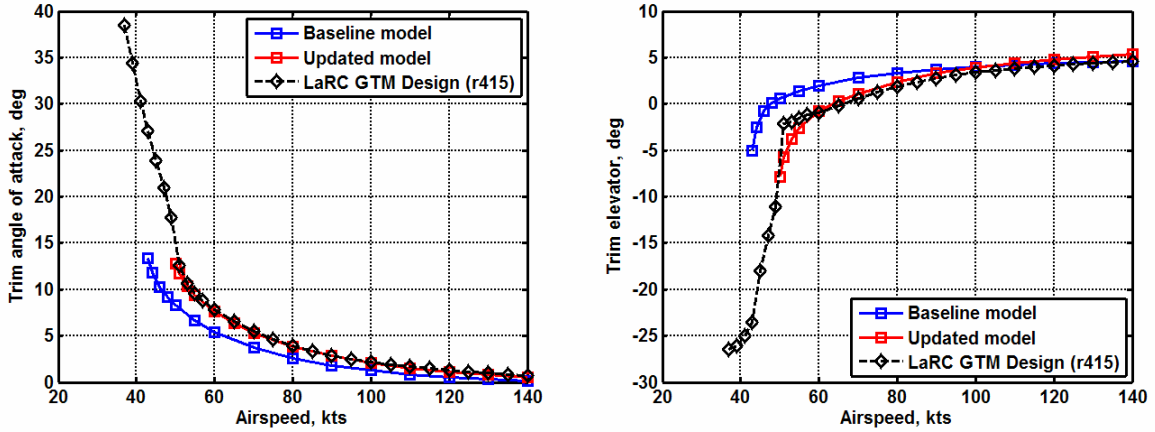

Figure 12. Comparison of Distributed Loading and LaRC GTM Models for Level Flight Trim.

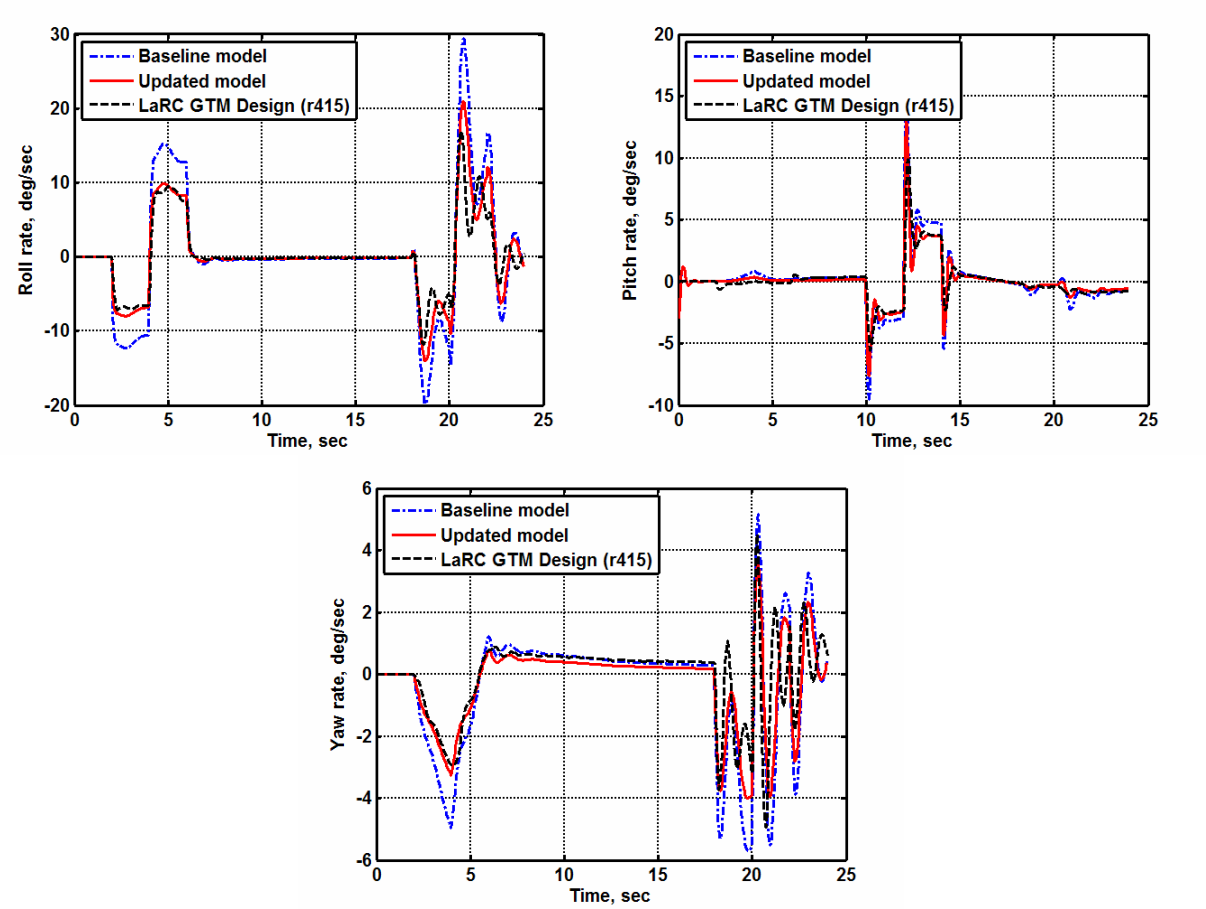

Figure 13. Comparison of Distributed Loading and LaRC GTM Models Aileron, Elevator, and Rudder Doublet Input Response Characteristics.

C. Lifting Surface Damage Effects

An objective has been to develop and apply a generic procedure for evaluating the impact of aircraft degradation on the dynamic flight envelope. This procedure for aerodynamic degradation modeling and envelope prediction was applied to lifting surface damage effects. Damage effects have been represented as alterations to the baseline geometric configuration, although more general application should account for localized changes in the sectional aerodynamic characteristics, such as reduction of the effectiveness of a partially damaged control surface. These effects are currently included and would require a more refined aerodynamic model to be implemented.

Lifting surface damage effects are implemented in the distributed loading aerodynamic model as follows. For a given damage condition, parameterized in terms of a tip loss fraction, affected segments in the distributed loading formulation are identified and the corresponding distributed aerodynamic loads are adjusted based on a load reduction factor determined from the effective segment area. This approach allows for a continuous variation in the extent of the damaged surface, as well as allowing for localized effects, such as a hole in the lifting surface, in an approximate sense. Note that only the aerodynamic effects associated with damage to the lifting surfaces have been considered in results presented in this paper. Inertial effects, including center of gravity shift and change to the aircraft mass properties, have not been modeled but may be incorporated following the approach outlined in Ref. 26.

This modeling approach was applied to the updated GTM distributed loading model and exercised for several hypothetical aircraft damage scenarios. Representative results illustrating the response due to instantaneous loss of the horizontal stabilizer tip are shown in Fig. 14. For these results, the aircraft is initially in a 70-knot level flight trim condition, and at 7 seconds into the simulation, the left outboard section of the horizontal tail is removed. No pilot recovery actions are applied following the damage condition. The effects of larger damage extents can be seen primarily as an increased reduction of damping of the short period mode, in addition to more significant coupling with the lateral-directional modes. Damage scenarios with wing damage have also been examined, with greater coupling between longitudinal and lateral-directional motions observed.

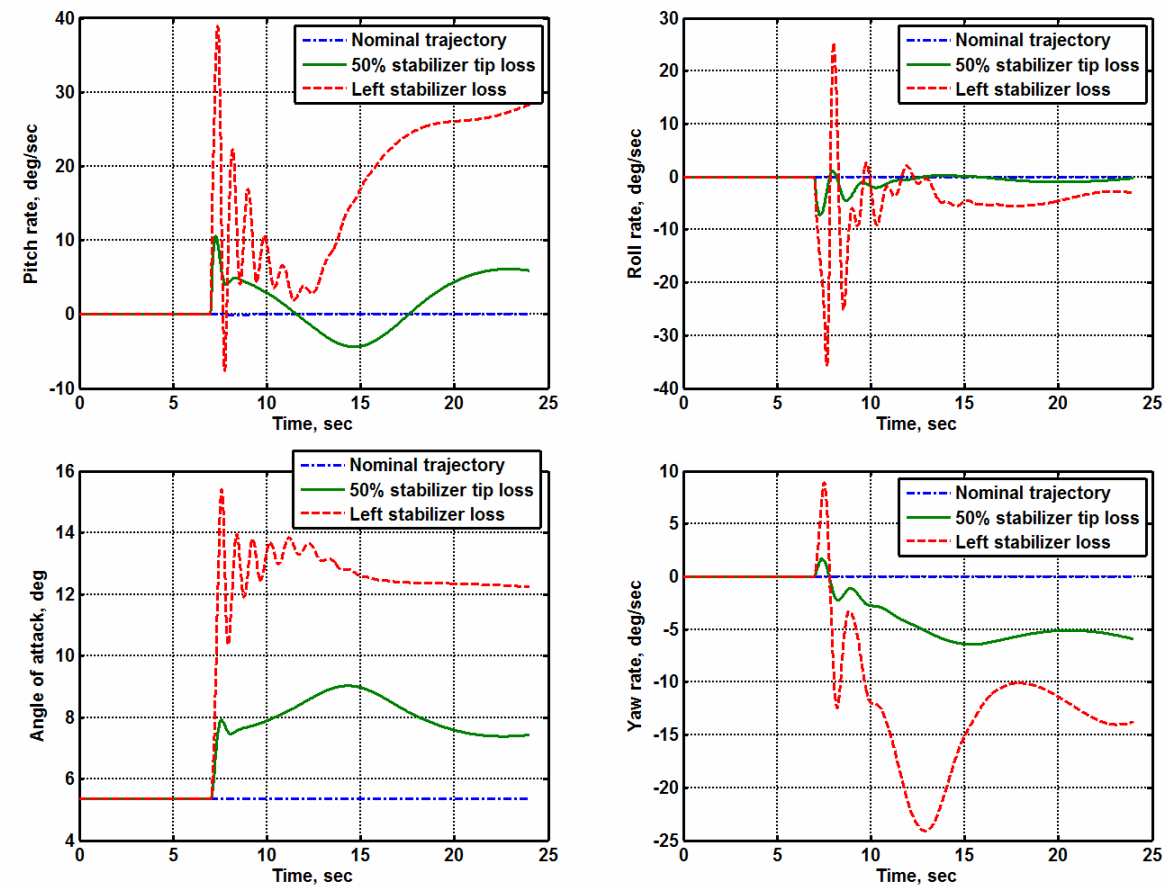

Figure 14. Response Characteristics Following Instantaneous Damage (Tip Loss) to the Left Horizontal Stabilizer for GTM Distributed Loading Simulation in 70 kts Level Flight.

Additional benchmarking has been performed for the distributed loading lifting surface damage model. Comparisons have been made with wind tunnel data for Ref. 27. The nature of the published data prevents direct correlation with model predictions. Instead, an alternative procedure is used to benchmark the distributed loading lifting surface damage model. Using similar modeling assumptions for the development of the generic distributed loading aerodynamic model, simplified analytical relationships for the lift curve reduction due to wing damage and pitch damping (short period stability) reduction due to horizontal stabilizer damage have been developed and are compared to wind tunnel data in Figs. 15 and 16, respectively. These analytical relationships have been developed using similar assumptions incorporated into the distributed loading model formulation. Agreement between model and data is relatively good for small damage extents, with better correlation observed for tail damage effects. Discrepancies between the predicted and observed lift curve reduction due to wing damage (Fig. 15) are likely due to approximations in representing non-uniform induced velocity effects. Discrepancies in the pitch damping (Fig. 16) may be cause by end-plating effects (which amount to a non-uniform interference effect between fuselage and tail surfaces) that are not modeled in the simplified analysis. These discrepancies may be addressed using improved aerodynamic modeling methods, such as vortex lattice models.

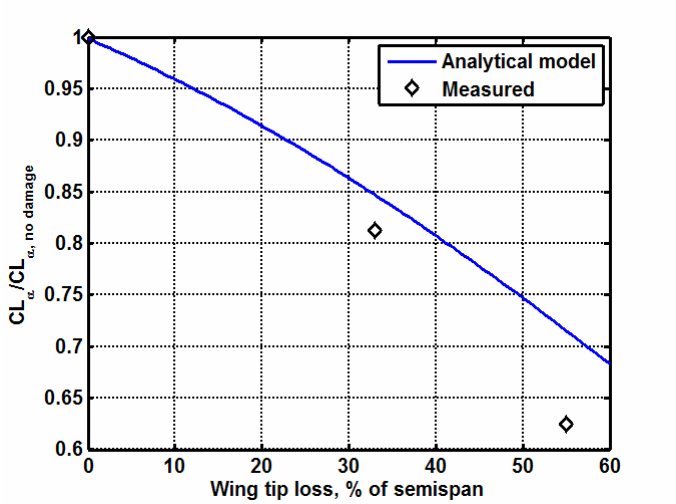

Figure 15. Comparison of Simplified Analytical Wing Damage Effects Model for Aircraft Lift Curve Reduction with Wind Tunnel Data (from Ref. 27)

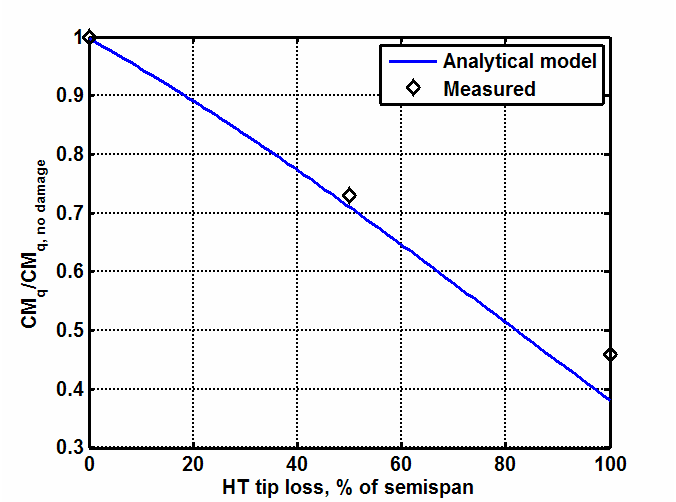

Figure 16. Comparison of Simplified Analytical Horizontal Tail Damage Effects Model for Aircraft Pitch Damping Reduction with Wind Tunnel Data (from Ref. 27)

D. Flight Envelope Determination

To determine the flight envelope of an aircraft, including accounting for degradation, it is necessary to consider several physical phenomena and limiting effects, including aerodynamic, structural and performance limits, controllability requirements, and stability margins, in addition to aircraft degradation effects. These effects need to be captured by the model and/or supporting data.

To formulate the problem of the dynamic envelope determination in mathematical terms, a generalized solution procedure was identified to determine the achievable operational range of an aircraft, given its current aerodynamic, flight dynamic, and structural configuration, in addition to limits on the control range and aircraft state. One approach to this problem is the determination of the achievable aircraft trim conditions, in addition to the inclusion of provisions for maneuvering effects, given limits on the controls and aircraft state. This solution to the dynamic flight envelope determination has been examined in this investigation using a numerical solution for the generic aircraft trim problem[28,29]. A summary of the solution approach is outlined in the following steps:

1. The target aircraft (degraded) configuration and flight condition is specified, which is defined in terms of the aircraft velocity, flight path angle, and sideslip angle. Steady maneuvering conditions (load factor, turn rate) may also be considered.

2. The aircraft control positions (surface deflections) and attitude are determined that result in non-accelerating flight (body-axis referenced). This solution is performed subject to aircraft limits, including the kinematic and dynamic constraints implicit to the aircraft model.
3. The aircraft operational limits (dynamic envelope) are defined from trim maps that span the performance, control, and/or structural limit constraints to the general trim solution.

This procedure for determining the dynamic flight envelope has been formulated in a series of Matlab functions.

Application of this procedure was performed for the GTM aircraft subject to degradation resulting from damage to the aircraft lifting surfaces (wing and horizontal stabilizer). Results were derived from the distributed loading model with lifting surface damage effects. Figure 17 illustrates the results of the dynamic envelope calculation procedure for the GTM model with increasing wing damage extents, which is expressed as the percentage of the wing tip removed (100% damage is equivalent to the entire left/right wing panel removed). In this result, the minimum flight speed has been determined as required for maintaining steady level trimmed flight, providing representative results illustrating the effects of wing damage on the minimum flight speed envelope. As the wing damage extent is progressively increased, it is necessary to apply aileron to counter the asymmetric roll moment on the aircraft. For small damage extents, the required aileron input is well within the control margin so that the minimum airspeed is determined by the aerodynamic stall limit, which was applied in this calculation by limiting the aircraft angle of attack. As the wing damage extent is increased, maintaining level trimmed flight is limited by the aileron control capability, which occurs for damage extents greater than 30%. Level trimmed flight conditions can be maintained by higher flight velocities, although allowance for non-zero sideslip angles will also affect the minimum flight speed. As noted in Ref. 27, the envelope for safe landing subject to wing damage is bounded by stall, roll control, and landing speed requirements; the boundary shown in Fig. 17 considers all but the landing speed operational limit.

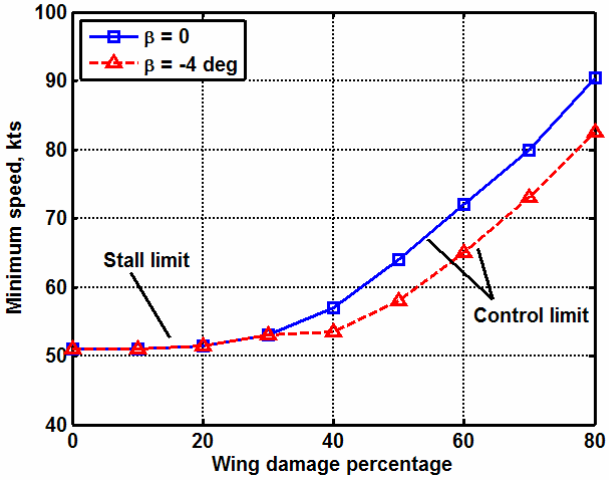

Figure 17. Minimum Flight Speed for GTM Distributed Loading Model Including Angle of Attack (Stall) and Wing Damage Control Authority Limits

Note that the wing damage minimum flight speed envelope in Fig. 17 has been determined assuming all lateral control is available for maintaining trimmed flight. Thus, this boundary is overly optimistic, and in general, control margin should be included for maneuvering and/or gust rejection. Envelope restrictions due to horizontal tail damage also have been examined, and it was found that damage to the stabilizer does not introduce additional performance or controllability limits as with the case of wing damage. While horizontal tail loss requires an increase in the required elevator and introduces an asymmetric condition that must be balanced by aileron/rudder deflections, no additional state/control limits are approached other than low speed stall limits. Consideration of stability limits (i.e., static margins and damping) has not been factored into the present analytical results, although these limits can be incorporated into the analysis as additional inequality constraints.

Determination of dynamic flight envelope limits as described above is computationally intensive, and direct calculation of these limits may be incompatible within an on-board envelope estimation system. Given that these envelope reductions may be parameterized (i.e., determined as a function of wing/tail surface damage extents), an on-board system can be implemented using pre-computed maps that are used in conjunction with an on-board detection system to identify and diagnose the nature and extent of aircraft aerodynamic performance degradation. These aspects are discussed in more detail in the following section.

E. Generalized Aerodynamic Performance Degradation Detection

On-board estimation of envelope restrictions subject to system/subsystem degradation by means of direct calculation likely will require parameterization of potential envelope restrictions in terms of physical metrics, such as wing damage extent as illustrated in the previous section. Thus, implementation of an on-board envelope (limit)

estimation system can be reduced to identifying and quantifying the degradation location and extent with an algorithmic approach.

Use of the detection filter approach has been proven to be an effective technique for failure detection and isolation when the desired fault modes can be expressed as additive disturbances to the system. Its application, however, becomes more complicated when the failures to be isolated are parametric variations in the system dynamics (i.e., multiplicative disturbances, Ref. 6). This complication arises for the case of aircraft lifting surface damage detection and isolation. Furthermore, relating the detection filter output (residuals) to the physical damage extent may not be straightforward. For these reasons, an alternative approach to aerodynamic performance monitoring and degradation detection has been considered.

A generalized aerodynamic performance degradation monitoring scheme, specifically one that can diagnose degradation sufficiently to permit estimation of flight envelope restrictions, has been investigated. To provide a direct relationship with the physical mechanisms (e.g., controllability margins) affecting the flight envelope boundaries, a reasonable starting point in formulating a detection scheme is derived from the aerodynamic loading applied to the aircraft during flight. A notional aerodynamic performance monitoring system is illustrated schematically in Fig. 18. Conceptually, this approach consists of the following steps:

1. The aircraft state and external loads are estimated from available flight data measurements using a nonlinear recursive estimator with augmented states representing the aircraft forces and moments.
2. Since the external forces include both aerodynamic and propulsive loads, propulsive forces (engine thrust) are removed from the estimated loads, which can be determined from monitored engine parameters, which is a common approach for flight data analysis[30].
3. The aircraft state estimate is used to determine the ideal aerodynamic forces/moments based on a non-degraded reference model, based on conventional stability derivatives or the distributed loading model formulation.
4. Aerodynamic degradation is determined by examining the difference between the estimated and reference model loads. Differences between estimated and reference model loads (referred to as residual loads) provide an indication of the degradation location and extent. This approach is conceptually similar to a model-based monitoring system for detecting thruster leakage failures in a spacecraft application[31].
5. The output from the detection scheme is a residual vector that provides an indication of the aircraft aerodynamic degradation source and extent. This residual output is structured to be correlated with physical parameters characterizing the aerodynamic degradation so that pre-determined flight envelope limits may be imposed.

To detect aerodynamic degradation and to provide a method to relate output from the detection scheme to physical parameters characterization the degradation source, it was necessary to focus on the approach used for residual generation. In particular, the preferred residual generation scheme would ideally show reduced sensitivity to variations in the aircraft state. A residual generation scheme has been developed that adopts a "geometric"

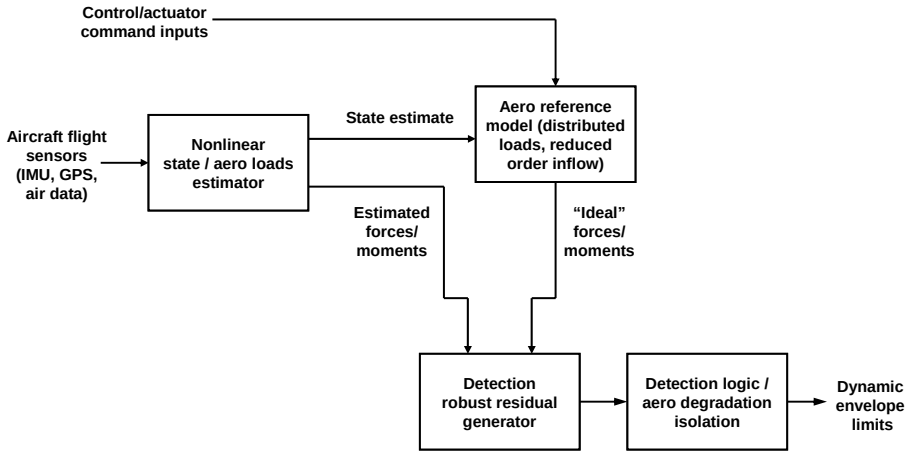

Figure 18. Schematic Illustration of Generalized Aerodynamic Performance Monitoring and Degradation Detection/Isolation Method.

approach loosely based on one interpretation of the FDF (UDF) design approach. The approach used determines the residual vector components based on the residual loads, which allows the output to be correlated with the physical source of degradation.

The aerodynamic degradation/residual generation scheme was applied to the identification of wing and horizontal tail damage extents based on flight measurements. The residual generation output was given as two residuals (indicated as r_1 and r_2), which may be used to infer the damage location and extent. Concept evaluations were performed using the simulation model described previously. Results are shown with this detection scheme in Fig. 19 for simulations of horizontal tail damage. For results given in Fig. 19 (as well as Figs. 20 and 21), the line type is used to denote the residual vector component response while the line color is used to denote the damage extent. Also shown in Fig. 19 are the corresponding angle of attack time histories (again these simulations have been performed with no corrective inputs made, which generally results in larger angle of attack excursions than if a pilot were in the simulation loop). Examination of the simulation results shows that the r_2 residual maintains a nearly constant value during tail damage scenarios that is independent of the damage extent, while the r_1 residual increases proportionally with damage extent. For wing damage simulations (Fig. 20), the opposite behavior is observed where the r_1 residual remains fixed and the r_2 residual increases with damage extent. Figure 21 also shows that damage to the opposite wing results in a sign change of the r_1 residual while the magnitude of the residuals remains unchanged for identical wing damage extents.

The magnitude of the r_1 and r_2 residuals during degraded conditions is such that simple logic may be used to diagnose both the damage location (left/right wing or horizontal tail) and damage extent. Although it has not been considered directly, it is anticipated that vertical tail damage may be incorporated by including a third residual output. Additional considerations for implementation in an on-board system are discussed below.

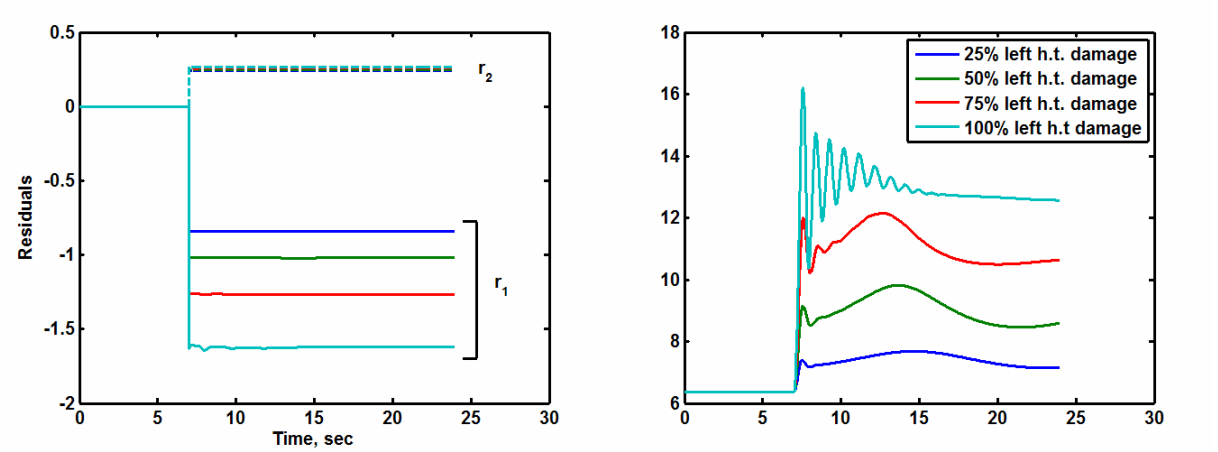

Figure 19. Aircraft Damage Detection and Diagnostic Algorithm Output and Corresponding Angle of Attack Response for Simulated Tail Damage Scenarios.

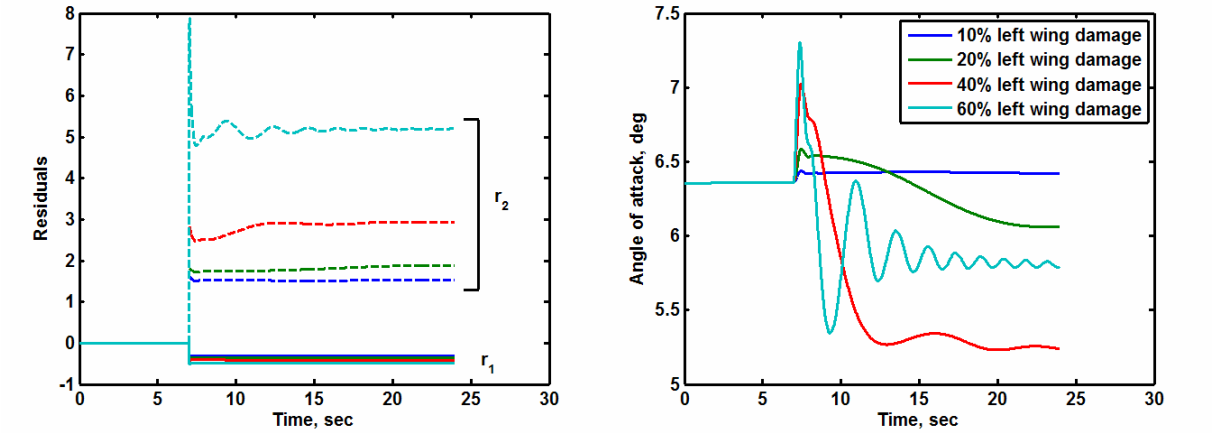

Figure 20. Aircraft Damage Detection and Diagnostic Algorithm Output and Angle of Attack Response for Simulated Left Wing Damage Scenarios.

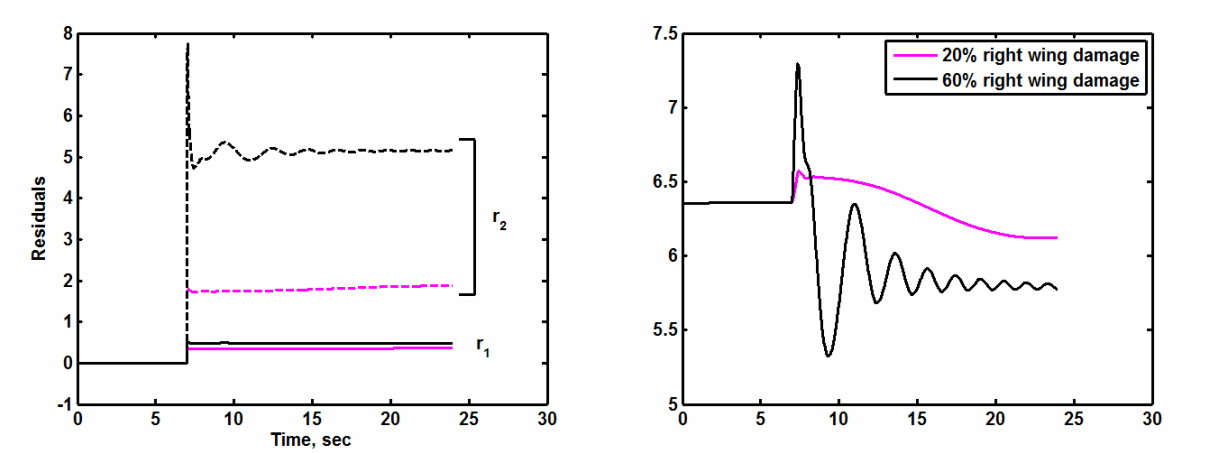

Figure 21. Aircraft Damage Detection and Diagnostic Algorithm Output and Angle of Attack Response for Simulated Right Wing Damage Scenarios.

F. On-board Implementation Considerations

On-board implementation of the aerodynamic performance/degradation monitor requires an estimator for determining the applied (aerodynamic) loads on the aircraft, which feeds the residual generation process used for fault detection and isolation. Estimation of the aircraft state and aerodynamic forces/moments can be performed using a nonlinear, model-based recursive estimator with an augmented state model including aircraft motion states in combination with additional states for the forces and moments. An approach such as this is not uncommon, having been used previously in aircraft system identification studies (e.g., the Estimation-Before-Modeling method[32]).

Initial evaluations used an extended Kalman filter (EKF) for the nonlinear state/loads estimation. In general, performance of the EKF estimator is sensitive to many aspects of the model formulation and assumed statistical properties of the system disturbance and noise. Representation of aircraft attitude presents another aspect of the EKF implementation. The EKF formulation for initial investigations used Euler angles for aircraft attitude, resulting in an 18th order model including aircraft inertial position (3 states), inertial velocity (3 states), Euler angle vector (3 states), and body-axis angular rates (3 states). The state vector was augmented by the specific forces and moments on the aircraft (6 states), which are modeled as first-order Gauss-Markov processes. Since specific moments were including in the estimator, the state propagation was nonlinear to account for the rigid body inertial couplings. The extended Kalman filter was implemented using a continuous-discrete update algorithm where state and covariance propagation was performed using a continuous model while measurement updates were done as a discrete, sampled-data process[33]. This approach permitted measurement updates at different rates, which was needed for the current application.

The EKF-based nonlinear estimator was coupled with the aerodynamic degradation detection scheme to provide an assessment of the overall system performance in an application representative of an on-board envelope estimation system. Simulations have been performed to evaluate the residual generation/detection scheme using noise contaminated vehicle response measurements with (simulated) sensor output representative of a modern commercial transport aircraft. Parameters for the simulation measurement model (i.e., measurement rates and accuracies) were chosen to be representative of a commercial IMU/GPS system based on separate flight test results. Results showing the performance of the residual generation/detection scheme using estimated loads are shown in Figs. 22 through 24, which illustrate the residual output based on an "ideal" reference model, i.e., aerodynamic loads are determined using the distributed loading model with simplified (and corrected) momentum inflow model driven by the true aircraft states. Figure 22 presents the residual generation/detection scheme output using estimated loads and ideal reference model for 40% wing tip loss damage scenario. The residual vector components, denoted by solid lines, show the presence of noise contamination, but the trends track the theoretical response (shown by the dashed lines in Fig. 22). Note that the r_1 residual component, which maintains a constant value for wing damage, shows less noise sensitivity than the r_2 residual. This characteristic is highly desirable from a fault detection/isolation perspective (i.e., it is more important to isolate the damage location first prior to determining the damage extent). Similar results are shown in Figs. 23 and 24 illustrating horizontal tail damage scenarios. Again, the presence of noise contamination can be seen, but the residual components track the theoretical trends.

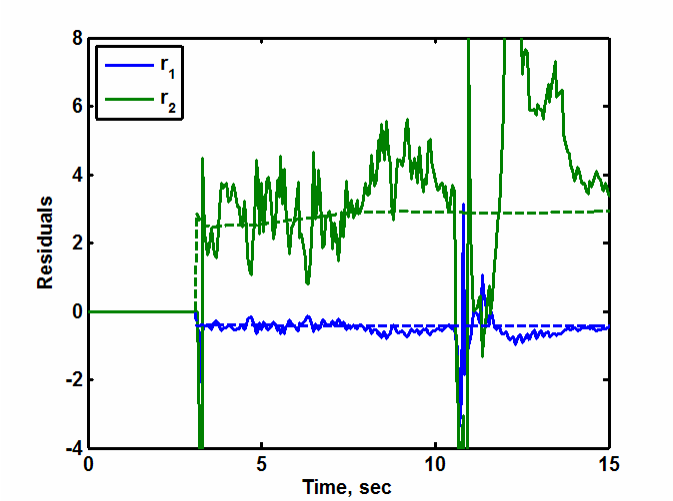

Figure 22. Residual Generation/Detection Scheme Output for Wing Damage Scenario (40% Left Tip Loss), EKF Estimated Loads and Ideal Reference Model.

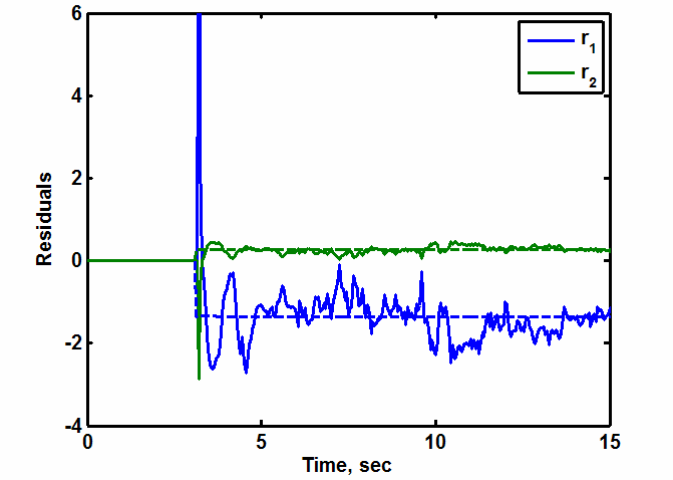

Figure 23. Residual Generation/Detection Scheme Output for Horizontal Tail Damage Scenario (80% Left Tip Loss), EKF Estimated Loads and Ideal Reference Model.

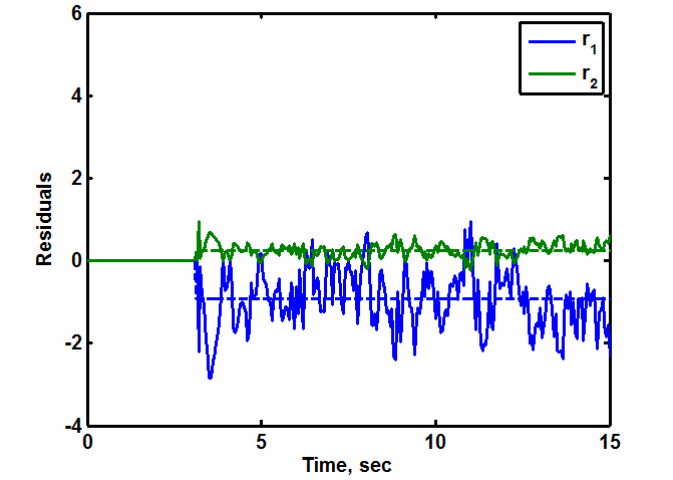

Figure 24. Residual Generation/Detection Scheme Output for Horizontal Tail Damage Scenario (40% Left Tip Loss), EKF Estimated Loads and Ideal Reference Model.

These results show promise of the aerodynamic performance degradation detection/isolation methods described previously. Note that the "glitch" observed in the r_2 residual component response at approximately 11 seconds into the simulation shown in Figure 22 can be traced to the EKF output and is caused by tracking of the heading measurement, which switches from -180 to 180 degrees. Simulation results using the estimated states in the reference model calculation indicated deterioration in detection performance, which can also be traced back to the presence of inconsistencies in the state estimated. These issues indicate that detection performance may be improved with an alternative nonlinear estimation scheme. Work is continuing to evaluate measurement signal-to-noise sensitivity on the ability to perform fault detection/isolation using the generalized scheme. In addition, the application of robust residual generation methods[6] should provide a method to further reduce the sensitivity to measurement noise. These extensions will be addressed in future work.

V. Concluding Remarks

This paper describes methods for identifying aerodynamic performance degradation and assessing the impacts of degradation on the dynamic flight envelope, with emphasis placed on the on-board implementation of the envelope estimation system. Such a system notionally would perform outer-loop supervision for an aircraft to augment adaptive/envelope limiting control systems and/or to provide inputs for intelligent guidance flight directors to provide safe landing in the presence of aircraft impairment (e.g., failed control surfaces, lifting surface damage, and icing). Results are provided that demonstrate elements of the overall envelope estimation system and highlight areas for further development leading to an on-board system implementation and demonstration.

Determination of the aircraft flight envelope, including accounting for the effects of aerodynamic performance degradation, can be performed using analytical methods outlined in this paper. Computational requirements, however, are such that any operational limits due to aerodynamic degradation need to be evaluated parametrically when implementing an on-board envelope estimation system. Thus, an essential element for implementation of an on-board system is the development of methods for the detection of aerodynamic degradation that may be correlated with physical parameters. Model-based fault detection methods, such as the FDF, provide one approach to identify and isolate both component failures and performance degradation, including the onset of upset conditions as shown through evaluations with flight test data for a small unmanned aircraft. Requirements for an on-board envelope estimation system have led to the investigation of a generalized approach for aerodynamic performance degradation detection. This generalized approach has been applied to the detection of wing/tail lifting surface damage. Results presented in this paper show promise of the generalized approach for isolating wing/tail damage extents, as shown through evaluations with simulated noise contaminated measurements. Further developments are required to improve noise robustness properties of the detection scheme.

Acknowledgments

This work was supported through a NASA SBIR Phase I research study (Contract No. NNX09CE91P), with Dr. Sungwan Kim serving as the Contracting Officer's Technical Representative. Flight test results for the UDF demonstration were supported through a separate NASA SBIR Phase I research study (Contract No. NNL07AA63P), with Mr. Kenneth Goodrich serving as the Contracting Officer's Technical Representative.

References

[1]Federal Aviation Administration, "Airplane Upset Recovery Training Aid, Revision 1," available from http://www.faa.gov/avr/afs/afs200/afs210/index.cfm, August 2004.

[2]Boeing Corporation, "Statistical Summary of Commercial Jet Airplane Accidents Worldwide Operations 1959-2005," Aviation Safety, Boeing Commercial Airplanes, May 2006.

[3]Belcastro, C.M. and Belcastro, C.M., "Application of Failure Detection, Identification, and Accommodation Methods for Improved Aircraft Safety," Proceedings of the American Control Conference, Arlington, VA, June 2001.

[4]Shin, J.Y., "Parameter Transient Behavior Analysis on Fault Tolerant Control System," NASA CR-2003-212682, December 2003.

[5]Croft, J.W., "Refuse-to-crash: NASA Tackles Loss of Control," Aerospace America, March 2003.

[6]Hwang, I., Kim, S, Kim, Y., and Seah, C.E., "A Survey of Fault Detection, Identification, and Reconfiguration Methods," to appear in the IEEE Transactions on Control Systems Technology, accepted for publication June 2009.

[7]Horn, J., Calise, A.J., Prasad, J.V.R., and O'Rourke, M., "Flight Envelope Cueing on a Tilt-rotor Aircraft Using Neural Network Limit Prediction," American Helicopter Society 54th Annual Forum, Washington D.C., May 1998.

[8]Merret J.M., Hossain, K.N., and Bragg, M.B., "Envelope Protection and Atmospheric Disturbances in Icing Encounters," AIAA 2002-0814, January 2002.

[9]Gingras, D.R., Barnhart, B., Ranaudo, R., Ratvasky, T.P., and Morelli, E., "Envelope Protection for In-flight Ice Contamination," AIAA 2009-1458, January 2009.

[10]Bosworth, J.T. and Williams-Hayes, P.S., "Flight Test Results from the NF-15B Intelligent Flight Control System (IFCS) Project with Adaptation to a Simulated Stabilator Failure," AIAA 2007-2818, May 2007.

[11]Bosworth, J.T., "Flight Results of the NF-15B Intelligent Flight Control System (IFCS) Aircraft with Adaptation to a Longitudinally Destabilized Plant," AIAA 2008-6985, August 2008.

[12]Beard, R., "Failure Accommodation in Linear Systems through Self-Reorganization," Rept. MVT-71-1, Man Vehicle Laboratory, M.I.T., Cambridge, MA, 1971.

[13]Jones, H., "Failure Detection in Linear Systems," Ph.D. Thesis, Dept. of Aeronautics and Astronautics, M.I.T., Cambridge, MA, 1973.

[14]Meserole, J. S., Jr., "Detection Filters for Fault-Tolerant Control of Turbofan Engines," Ph. D. Thesis, Dept. of Aeronautics and Astronautics, M.I.T., Cambridge, MA, June 1981.

[15]Bundick, W.T., "A Preliminary Design of a Failure Detection Filter for Detecting and Identifying Control Element Failures in a Transport Aircraft," NASA TM 87576, July 1985.

[16]Massoumnia, M.A., "A Geometric Approach to the Synthesis of Failure Detection Filters," *IEEE Transactions on Automatic Control*, Vol. AC-31, (9), September 1986, pp. 839-846.

[17]Chung, W.H. and Speyer, J.L., "A Game Theoretic Fault Detection Filter," *IEEE Transactions on Automatic Control*, Vol. 43, (2), February 1998, pp. 143-161.

[18]Douglas, R.K. and Speyer, J.L., "H_∞ Bounded Fault Detection Filter," *Journal of Guidance, Control, and Dynamics*, Vol. 22, (1), January-February 1999, pp. 129-138.

[19]Miller, R. and Ribbens, W., "Detection of the Loss of Elevator Effectiveness Due to Aircraft Icing," AIAA Paper 99-0637, Proceedings of the 37th AIAA Aerospace Sciences Meeting, Reno, NV, January 1999.

[20]McKillip, R.M., Jr., "Aircraft Icing Detection System", U.S. Patent No. 6,304,194, October 16, 2001.

[21]McKillip, R.M., Jr. and Keller, J.D., "Algorithmic Icing Detection for the V-22 Osprey," presented at the American Helicopter Society Flight Controls and Crew Systems Design Specialists' Meeting, Philadelphia, PA, October 2002.

[22]Keller, J.D., McKillip, R.M., Jr., and Wachspress, D.A., "Physical Modeling of Aircraft Upsets for Real Time Simulation Applications," AIAA 2008-6205, AIAA Atmospheric Flight Mechanics Conference, Honolulu, HI, August 2008.

[23]Wise, J., "Austin and Goliath," *Popular Science*, Vol. 263, (2), August 2003.

[24]Corrigan, J.J., Meyer, A., Bothwell, M., and Brown, H., "Computer Flight Testing of Rotorcraft," presented at the American Helicopter Society Vertical Lift Aircraft Design Conference, San Francisco, CA, January 2006.

[25]Howlett, J.J., "UH-60A Black Hawk Engineering Simulation Program: Volume I – Mathematical Model," NASA CR-166309, December 1981.

[26]Bacon, B.J. and Gregory, I.M., "General Equations of Motion for a Damaged Asymmetric Aircraft," AIAA 2007-6306, AIAA Atmospheric Flight Mechanics Conference, Hilton Head, SC, August 2007.

[27]Shah, G.H., "Aerodynamic Effects and Modeling of Damage to Transport Aircraft," AIAA-2008-6203, AIAA Atmospheric Flight Mechanics Conference, Honolulu, HI, August 2008.

[28]McFarland, R.E., "Trimming an Aircraft Model for Flight Simulation," NASA TM 89466, October 1987.

[29]De Marco, A., Duke, E.L., and Berndt, J.S., "A General Solution to the Aircraft Trim Problem," AIAA 2007-6703, AIAA Modeling and Simulation Technologies Conference, Hilton Head, SC, August 2007.

[30]Bach, R.E., Jr., "State Estimation Applications in Aircraft Flight Data Analysis," NASA RP 1252, March 1991.

[31]Lee, A.Y. and Brown, M.J., "A Model Based Thruster Leakage Monitor for the Cassini Spacecraft," Proceedings of the American Control Conference, Philadelphia, PA, June 1998.

[32]Sri-Jayantha, M. and Stengel, R.F., "Determination of Nonlinear Aerodynamic Coefficients Using the Estimation Before Modeling Method," *Journal of Aircraft*, Vol. 25, (9), September 1998.

[33]Gelb, A., *Applied Optimal Estimation*, MIT Press, 1974.